Chapter 7

The Electrochemical Performance of Deposited Manganese Oxide-Based Film as Electrode Material for Electrochemical Capacitor Application

Chan Pei Yi and Siti Rohana Majid

Additional information is available at the end of the chapter

http://dx.doi.org/10.5772/intechopen.71957

Abstract

The transition metal oxide has been recognized as one of the promising electrode materials for electrochemical capacitor application. Due to the participation of charge transfer reactions, the capacitance offered by transition metal oxide can be higher compared to double layer capacitance. The investigation on hydrous ruthenium oxide has revealed the surface redox reactions that contributed to the wide potential window shown on cyclic voltammetry curve. Although the performance of ruthenium oxide is impressive, its toxicity has limited itself from commercial application. Manganese oxide is a pseudocapacitive material behaves similar to ruthenium oxide. It consists of various oxidation states which allow the occurrence of redox reactions. It is also environmental friendly, low cost, and natural abundant. The charge storage of manganese oxide film takes into account of the redox reactions between Mn^{3+} and Mn^{4+} and can be accounted to two mechanisms. The first one involves the intercalation/deintercalation of electrolyte ions and/or protons upon reduction/oxidation processes. The second contributor for the charge storage is due to the surface adsorption of electrolyte ions on the electrode surface.

Keywords: pseudocapacitors, energy storage devices, metal oxides, thin films, electrode materials

1. Introduction

The electronics technologies we are granted nowadays are the results of many years' researches. From Benjamin Franklin, Alessandro Volta, Michael Faraday, and Nikola Tesla, the continuous efforts have developed the electrical knowledge which has been practicalized for the sake of living standards. The better quality of life and the transformation from agricultural-based economy into information-based economy indicating the globalization has taken place. Although the fruits of globalization are attractive, the globalization also causes unavoidable negative

consequence such as global warming. The increased concentration of greenhouse gases in the atmosphere is referred as the impact of human activities such as the burning of fossil fuel for transports and power electricity plants. It brings into our concern that an alternative energy source is required, at the same time solving the energy demand issue that caused by globalization is needed. It is therefore, necessary to improve the energy management. Energy storage system, as part of the energy management, receives tremendous attentions for this purpose.

Energy storage system is a big family comprising various energy storage devices, for example, solar cell, battery, electrochemical capacitor, and fuel cell, which can be used for specific applications, for instance, the employment of fuel cell-based system over gasoline engine in transportation [1]. By reducing the rated fuel cell power and controlling the energy loss, the fuel efficiency can be enhanced [2]. Another technique of energy management is by distributing the power onto different energy sources. For example, a hybrid system based on a polymer electrolyte membrane fuel cell and nickel-metal hydride battery has been evaluated for tramway in Spain [3]. Tsukahara and Kondo have inspected the prospective hybridizations of fuel cell with Li-ion battery and electric double layer capacitor (EDLC) to power the railway vehicles [4].

Apart from transportation, many portable electronic devices also supported by the battery, that is also an energy storage device. From nickel-cadmium battery, nickel-metal hydride battery, to Li-ion battery, the studies on batteries have never stopped. To date, there are more than 35,000 published papers regarding to lithium battery according to Web of Science. Nowadays, Li-ion battery is the most promising battery. A diagram describing charging-discharging mechanism of Li-ion battery is displayed in **Figure 1**.

As a rechargeable battery, Li-ion battery encourages a rapid growth in the mobile devices technology. Abraham has outlined the limitation and future outlook of Li-ion battery [5]. Li-O_2 or Li-air battery will be the battery that can achieve the utmost energy density. However, a down-to-earth Li-air battery is still well on the way to be practical. Recently, an all-solid-state rechargeable battery based on a solid glass electrolyte promises a safe, low cost, and longer cycle life properties for battery [6]. The performances of batteries are summarized in Ragone plot [7], **Figure 2**.

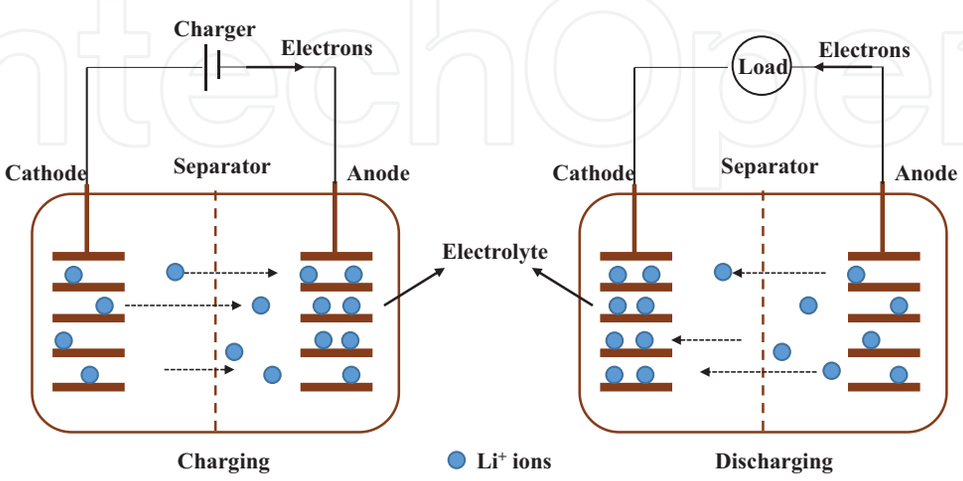

Figure 1. Charging-discharging schematic diagram of li-ion rechargeable battery.

http://dx.doi.org/10.5772/intechopen.71957

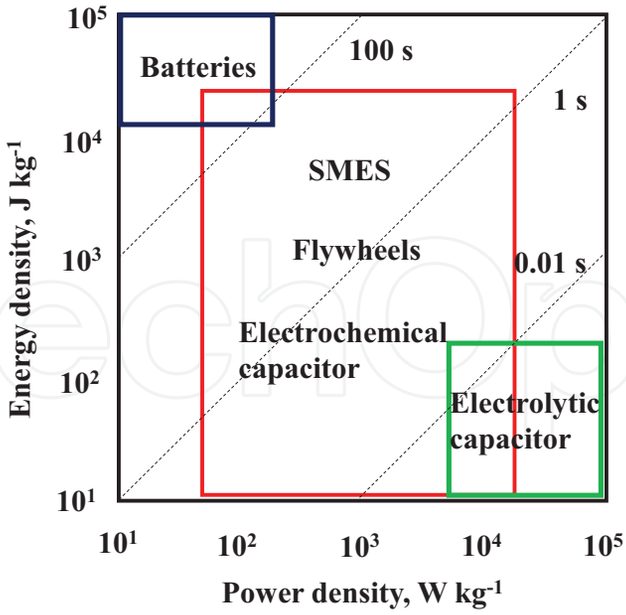

Figure 2. Ragone plot.

Nowadays, the Ragone plot, which is an indication of possible development for certain energy storage devices, has included some storage devices other than batteries. For example, fuel cell, capacitor, and supercapacitor. However, it does not show all the other important properties for instance cycle stability, temperature range of operation, and energy efficiency. Therefore, the Ragone plot cannot be the only reference for evaluating the performance of an energy storage device. Nevertheless, it can be used as a source of information which is continually updated and improved [8].

An electrochemical capacitor, also known as supercapacitor, is an energy storage device whereby its electrochemical performance lies in between a conventional capacitor and a battery. It can store larger amount of energy compared to a capacitor, but lesser when compared to a battery. Nonetheless, an electrochemical capacitor has higher power density than a battery. The electrochemical capacitor is categorized into two types: electric double layer capacitor (EDLC) and pseudocapacitor. The working principle behind an EDLC is based on the electrostatic interaction. The EDLC charges/discharges are according to the adsorption/de-adsorption processes. The schematic diagram of an EDLC is depicted in **Figure 3**.

As shown, the positive and negative charges are attracted to the electrode surfaces with opposite charges respectively. The charges are thus stored by means of the electric double layer formed at the electrode surface. Therefore, material with high surface area and conductivity such as carbon materials are suitable to be employed as electrode for EDLC. Conversely, a pseudocapacitor makes use of the charge transfer reactions for charge storage purpose. The corresponding capacitance is named as pseudocapacitance.

Although the charge storage mechanisms are different, the electrochemical signatures of EDLC and pseudocapacitor are similar when they are examined using cyclic voltammetry test [9]. As

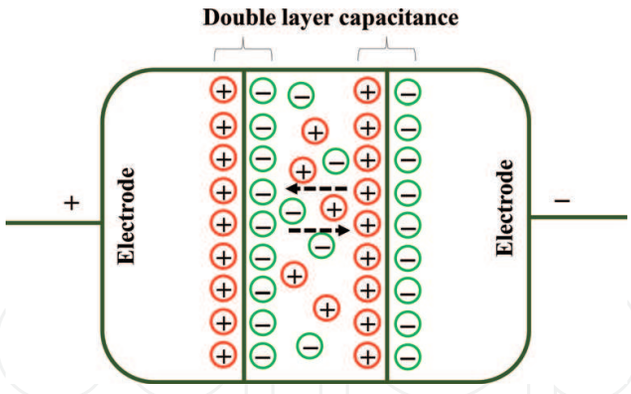

Figure 3. Schematic diagram of EDLC.

the charge stored is linearly dependent with the potential, the resultant voltammetry curve exhibits a rectangular and symmetry shape. The redox materials such as conducting polymers and transition metal oxides are usually studied as the potential electrode material for pseudocapacitor. The hydrous ruthenium oxide is found to exhibit a high specific capacitance of 720 F g^{-1}, making it a promising electrode material for electrochemical capacitor [10]. Nevertheless, ruthenium oxide is expensive and toxic. This has prevented hydrous ruthenium oxide from commercial use. Besides, the usage of strong acidic electrolyte also forbids it from application. Other materials such as SnO_2, MnO_2, TiO_2, VO_2, and MoO_3 have been studied as the alternative electrode material and they are showing different potentials for the practical applications [11–15]. Among the materials, manganese oxide has been widely studied due to the fact that the manganese oxide can form a variety of composites with different materials using various synthesis routes [16–18]. In the following section, we will discuss about the properties of manganese oxide.

2. Manganese oxide

Manganese is one of the most abundant elements on Earth which is widely distributed across the crust. In general, manganese deposit forms from seawater. Thus, its redox sensitivity toward oxidation state of ocean enables us to explore the ancient environmental conditions [19]. In human body, the manganese participates in carbohydrate metabolism as well as formation of bone and connective tissues. Manganese oxide has been used since ancient time. It was employed for elucidation of glass and acted as black pigment. Throughout the years, the researches on manganese oxide have deepen the understanding on the chemistry of this compound [20–26]. At the same time, the utilization of manganese oxide has been exploited and diversified.

The advantage of manganese oxide lies in the feasible formation of various structures based on different arrangements of basic building structure of manganese oxide, which is MnO_6 octahedral. This is a structure where O^{2-} ions are octahedrically coordinated to the central of Mn^{4+} ion, as shown in **Figure 4**.

http://dx.doi.org/10.5772/intechopen.71957

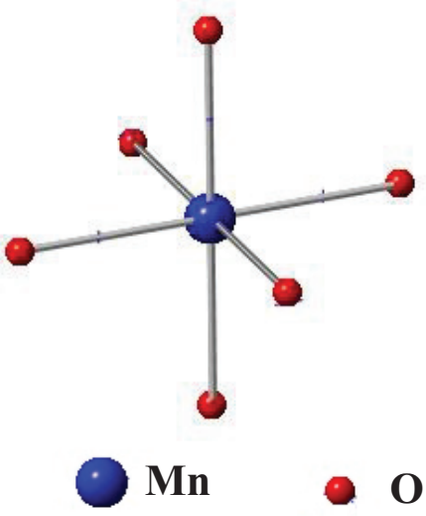

Figure 4. Schematic diagram of MnO_6 octahedral.

The octahedral structure can be arranged through edge- and/or corner-sharing. In common, there are two types of structure: (a) tunnel or chain structure and (b) layer structure. Chain structure is made up of corner-sharing arrangement while tunnel structure is resulted from the combination of single, double, or triple chains of MnO_6 octahedral. Layer structure is constructed by the sheets or layers stacking of MnO_6 octahedral. Both kinds of structure can hold proton and electrolyte cation.

As a transition metal, manganese exists in various valence states which in turns form a variety of mineral with distinct physical and chemical properties. When different phases of manganese oxide are mixed, they can intergrow to form a new structure. The manganese oxides mineral is inclusive of MnO_2, Mn_2O_3, Mn_3O_4, and MnOOH. The different forms of minerals are named as the polymorphs. For instance, MnO_2 has three polymorphs: pyrolusite, ramsdellite, and nautile while MnOOH has polymorphs of manganite, groutite, and feiknechtite. The polymorphic form is dependent on the linkage between MnO_6 octahedrals, which is determined by the preparation process of manganese oxide [27]. Over the years, the variation in structural forms and properties has made manganese oxide a suitable candidate for different applications such as energy storage system, biosensor, coating, environmental, and nuclear science [28–34]. According to Pourbaix diagram, **Figure 5**, the electrochemical performances of manganese oxides in aqueous media are arisen from its various oxidation states (Mn^{2+}, Mn^{3+}, and Mn^{4+}) that are emerged from different oxide phases (Mn_3O_4, Mn_2O_3, and MnO_2) which are thermodynamically stable in alkaline region [35].

In general, the charge storage of manganese oxide relies on two mechanisms: (a) surface adsorption of electrolyte ions and (b) intercalation/deintercalation of electrolyte ions and/or proton upon reduction/oxidation [36]. Although higher surface area can lead to higher value of specific capacitance, further increasing in surface area is found to not contribute

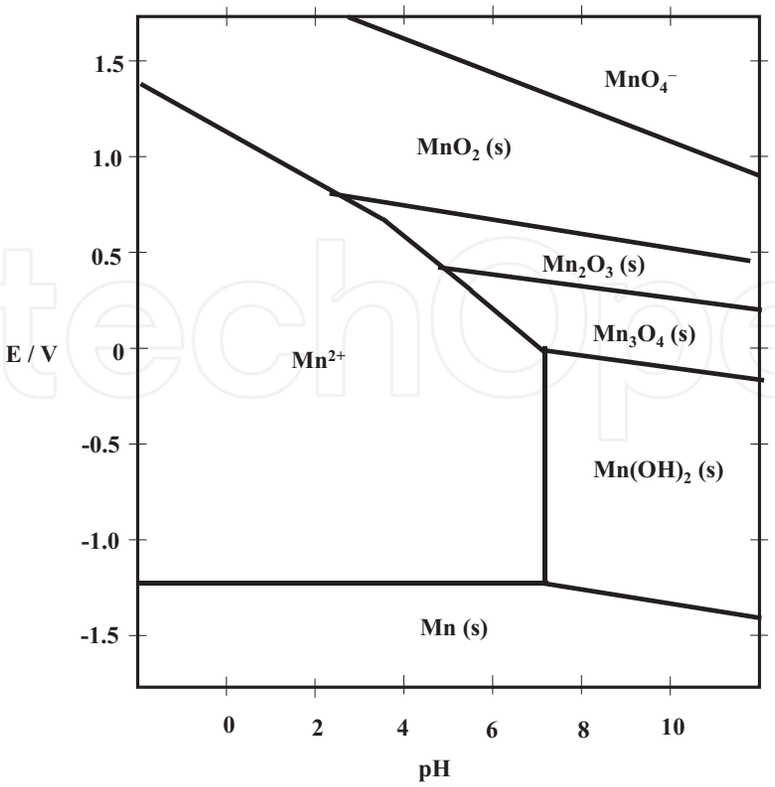

Figure 5. Pourbaix diagram of manganese.

to the specific capacitance [12, 37]. The structure of the manganese oxide can determine its electrochemical performance. A structure with more rooms for the insertion of electrolyte ions will offer higher charge storage capacity, and subsequently higher specific capacitance. To date, the researchers are still working best to figure out the charge storage mechanism of manganese oxide in order to better explain its electrochemical behavior [38–40]. This knowledge will inspire us and provide us a way on how to fully utilize the potential capacitance of manganese oxide.

Manganese oxide-based film can be prepared via a variety of methods. A material will exhibit different properties such as particle sizes and types of defects, depending on the fabrication routes. In addition to this, the change in experimental parameters also produces materials with different electrochemical properties. The common preparation methods are the hydrothermal, chemical bath deposition, polyol synthesis, sol–gel, electrodeposition, solvothermal, and co-precipitation [20, 36, 39, 41–45]. The specific capacitances obtained ranges from 121.5 to 698 F g^{-1}, which is still lower than the theoretical specific capacitance of manganese oxide (1380 F g^{-1}). To better utilize the electrochemical active sites, one should understand the relationship between the experimental method and the corresponding structure formed. This chapter will focus on the green and relatively simple method of electrodeposition. Thereafter, we will discuss about the electrochemical performance of manganese oxide-based film fabricated using electrodeposition technique.

http://dx.doi.org/10.5772/intechopen.71957

3. General principle of electrodeposition

Electrodeposition refers to an electrical process such as electrolytic and electrophoretic deposition, which allows the accumulated mass of a metal ions, or deposit, coated onto an electrode. A common configuration of electrodeposition is displayed in **Figure 6**.

It is usually made up of a working electrode, counter electrode, and reference electrode. The working electrode is the substrate where the deposition reaction takes place. The reference electrode is used to maintain the voltage stability for the working electrode while the counter electrode or auxiliary electrode is utilized to complete the current flow. There is various reference electrodes served for different electrolyte solutions. A standard hydrogen electrode (SHE) consists of 1.0 M H^+ (aq.) solution and is used to compare with other reference electrodes since the standard electrode potential of hydrogen is 0 V. Saturated calomel electrode (SCE) is a reference electrode composes of KCl solution and establishes based on the reaction between elemental mercury and mercury chloride. However, the dangerous nature of mercury content has prohibited the SCE reference electrode from widely use. Instead, the silver chloride (Ag/AgCl) electrode is employed. Ag/AgCl reference electrode is mostly utilized for electrochemical tests and industrial application due its simplicity for fabrication, stability, and non-toxicity. Nonetheless, the usage of Ag/AgCl in basic solution must be heedful because a long immersion of electrode allows the diffusion of OH^- ions into the internal filling solution, which can subsequently increase the pH and shift the reaction potential. The measurement of potential using various reference electrodes can be referred to SHE and the corresponding values are recorded in **Figure 7**.

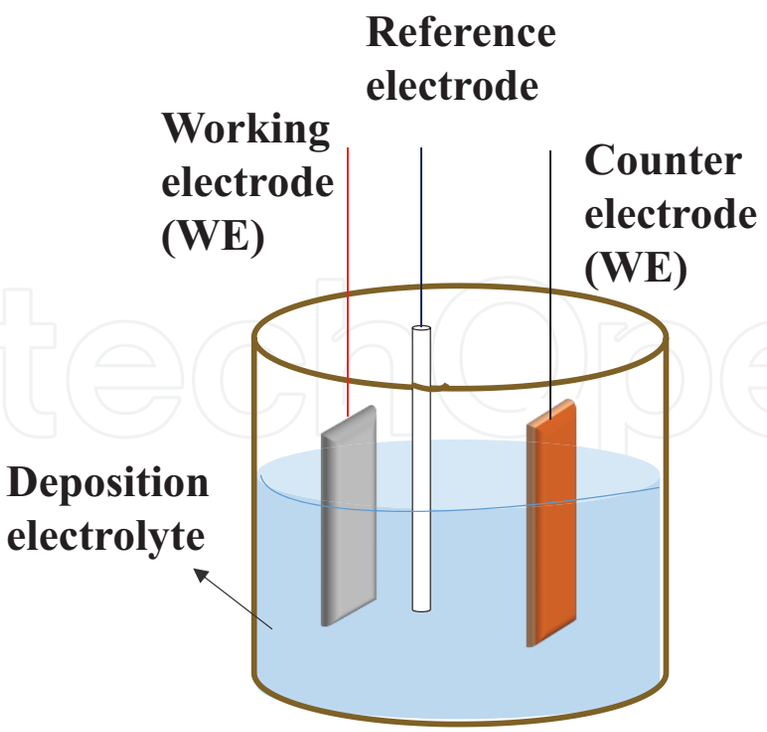

Figure 6. General electrodeposition setup.

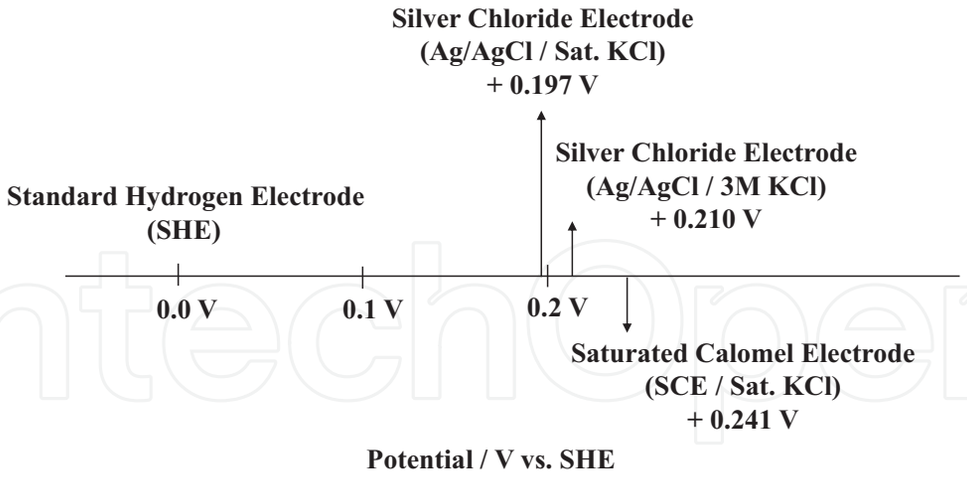

Figure 7. Voltage conversion between reference electrodes.

As electrolytic deposition makes use of solution containing metal ions for deposition purpose, electrophoretic deposition utilizes a mixture consists of suspended colloidal particles. Electrophoretic deposition was revealed when a Russian scientist observed the movement of clay particles in water induced by electric field. It occurs when the non-conductive electrically charged particles migrate to the electrode surface under an applied electric field. The charged particles suspend in the electrolyte due to the mutual electrostatic repulsion [46]. Inside the suspension, the surface charges attract the electrolyte ions with opposite charge. As a result, the counter ions adsorb onto the surface charges, forming a diffuse cloud of counter ions. The process is governed by electrostatic interaction. At the same time, the adsorbed ions repulse from each other. When they are close enough to overcome the electrostatic force, van der Waals attraction will be predominant and adhesion can occur. To achieve electrophoretic deposition, a stable suspension containing well-dispersed particles with desired electrophoretic mobility must be prepared firstly. The usage of additives such as dopamine and triethanolamine can help to stabilize the suspension [47–48]. In addition, it offers a more uniform and adherent deposit. The parameters that play the role on electrophoretic deposition are composition of dispersion medium, pH of electrolyte, and concentrations of particles and electrolyte. The principles behind electrolytic deposition and electrophoretic deposition have been studied [49–51]. An understanding about these two processes is required in order to fabricate desired electrode material. The oxidation kinetics of manganese oxide from Mn^{2+} is reliant on the deposition methods. Depends on the particle charge, electrodeposition can be divided into two types: anodic deposition and cathodic deposition. The anodic deposition is resulted from the oxidation of negative ions on anode (positively charged electrode). In contrast, the reduction of positive ions on cathode results in a cathodic deposition. For manganese oxide film, the anodic deposition involves the oxidation of cationic Mn^{2+} precursors while cathodic deposition is achieved by the reduction of anionic Mn^{7+} from MnO_4^-. Manganese (II) sulfate ($MnSO_4$), manganese (II) nitrate ($Mn(NO_3)_2$), manganese (II) acetate ($Mn(CH_3COO)_2$), and manganese (II) chloride ($MnCl_2$) can be used as precursors for Mn^{2+}. As the deposition mechanism is independent of precursors, it does not affect significantly on the capacitive behaviors of manganese oxides formed [52].

http://dx.doi.org/10.5772/intechopen.71957

Due to this reason, the mass loading plays an important role in determining the capacity of manganese oxide formed. Among these precursors, $Mn(CH_3COO)_2$ decomposes at lower potential and offers higher deposition rate which make it a favorable precursor. In addition, the Mn^{3+} is more stable with acetate compared to sulfate which makes it a thermodynamic favor for oxidation kinetics [53]. On the other hand, $KMnO_4$ is usually the Mn^{7+} precursor for cathodic deposition.

As the oxidation process can lead to the dissolution of metal substrate, the cathodic reduction is usually preferred over anodic oxidation as various metals can be employed as the substrates [51]. The anodic oxidation of Mn^{2+} involves other oxidation state of manganese ions. Initially the Mn^{2+} will diffuse and adsorb onto the electrode surface to form Mn_{ads}^{2+}. The adsorbed ions oxidize to Mn^{3+} which subsequently forms intermediate with water. Under appropriate heating temperature, the MnOOH intermediate can be transformed to MnO_2. The detailed oxidation reaction of Mn^{2+} to MnO_2 in the medium with different acidity is described in **Section 4** [54, 55]. According to Pourbaix diagram, the reduction process of Mn^{7+} occurs in a neutral aqueous solution is as follow, **Reaction 1** [35]:

$$MnO_4^- + 2H_2O + 3e^- \rightarrow MnO_2 + 4OH^- \quad (1)$$

The electrodeposition can be carried out either by a constant potential or current technique. For constant potential technique, the resulted current-time transient can be determined by following factors: (1) the potential and time of the oxide formation, (2) the potential and time of oxide reduction, and (3) the maintenance time of electrode at reversible potential before reduction takes place [56]. The chronopotentiometry is an electrodeposition technique performed with a constant current. The constant current is applied between working and auxiliary electrodes while the potential of working electrode is measured against a reference electrode. The potential reveals the reaction takes place on the electrode during the electrodeposition process. Before the electrodeposition starts, there is no concentration gradient of oxidants in the solution regardless of the distance from electrode surface. This initial potential is also called as open circuit potential. However, a concentration gradient of oxidants is formed when the reduction initiates by the application of current. The reduction is a resultant process of oxidants responds to the applied current. As a result, the oxidants near to the electrode surface are consumed, causing the oxidants diffuse from bulk solution toward electrode surface in order to accommodate the reduction process. The potential is comparable to the redox potential of certain electron transfer reaction. Since the concentration changes with time, this potential alters correspondingly. Once the current cannot be further sustained by this redox potential, which is due to the concentration of oxidants turns to zero, this potential will adjust to another redox potential in order to maintain the fixed current. The changing potential during galvanostatic deposition can lead to the formation of various morphologies. Different from chronoamperometry, which is a deposition method employing a constant voltage, a desired morphology can be formed accordingly. Knowledge of the interactions between electrode and electrodeposition parameters allows us to construct and improve the electrode film performance. Herein, the manganese oxide deposited using various deposition techniques are discussed and evaluated.

4. Electrochemical performance of deposited manganese oxide-based film

4.1. Effect of electrolyte composition

For anodic deposition, manganese acetate ($Mn(CH_3COO)_2$) and manganese sulfate ($MnSO_4$) are always chosen as the Mn^{2+} precursors. They offer different kinds of morphologies although the electrodeposition is carried out under the same conditions. For example, the morphology produced from 0.01 M $Mn(CH_3COO)_2$ at constant current density of 30 mA cm^{-2} exhibits interconnected but non-continuous nanorods structure, **Figure 8**(**a**) [57]. On the other hand, 0.01 M $MnSO_4$ leads to a continuous and homogenous nanorods structure (**Figure 8**(**b**)).

With the addition of H_2SO_4, a discrete crystallite of manganese oxide is formed ([58]). H_2SO_4 acts as a supporting electrolyte and enhances the stability of the soluble Mn^{3+} intermediate before further reactions [59]. This allows more manganese ions to be deposited and form a film on the substrate after certain electrodeposition time. The electrodeposition mechanism of manganese oxide with the presence of H_2SO_4 is shown as following [60]:

$$Mn^{2+} \rightarrow Mn^{3+} + e^{-} \tag{2}$$

Disproportionation pathway:

$$2Mn^{3+} \rightarrow Mn^{2+} + Mn^{4+} \tag{3}$$

$$Mn^{4+} + 2H_2O \rightarrow MnO_2 + 4H^{+} \tag{4}$$

Hydrolysis pathway:

$$Mn^{3+} + 2H_2O \rightarrow MnOOH + 3H^{+} \tag{5}$$

$$MnOOH \rightarrow MnO_2 + H^{+} + e^{-} \tag{6}$$

Depending on the concentration of acid, there are two proposed pathways for the formation of manganese oxide: disproportionation and hydrolysis. **Reaction 2** shows the oxidation of Mn^{2+} become soluble Mn^{3+} intermediate. If the supporting acid, which is H_2SO_4 in this case, has higher

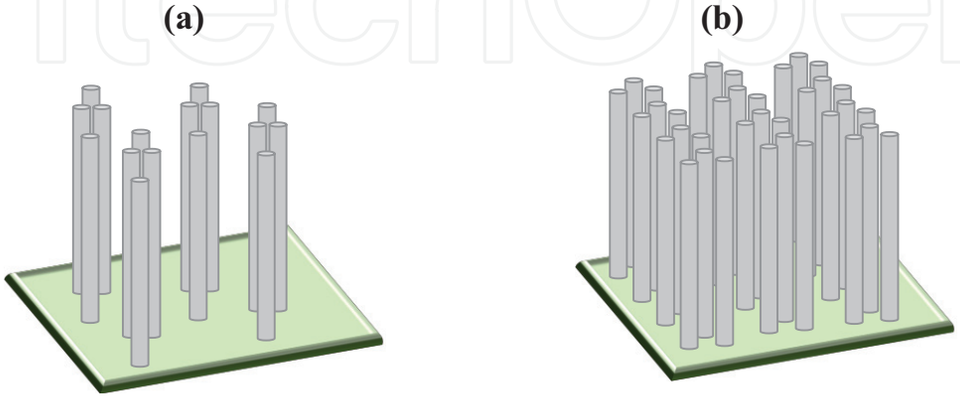

Figure 8. Formation of nanorods structure in (a) 0.01 M $Mn(CH_3COO)_2$ and (b) 0.01 M $MnSO_4$.

concentration, Mn^{3+} achieves relatively higher stability allowing it to experience disproportionation which subsequently forms Mn^{2+} and Mn^{4+} (**Reaction 3**). Mn^{4+} is then hydrolyzed to form MnO_2 on the surface of substrate (**Reaction 4**). On the other hand, at lower acidity condition, Mn^{3+} is less stable and thus can hydrolyze easily to form MnOOH (**Reaction 5**). MnOOH is then converted to MnO_2 under suitable annealing temperature (**Reaction 6**). The manganese oxide electrodeposited from the electrolyte containing H_2SO_4 can obtain specific capacitance as high as 5600 F g^{-1} [59]. A less acidic medium also can be achieved by adding sodium sulfate (Na_2SO_4). It can act as the supporting electrolyte for Mn^{2+} and Mn^{7+} precursors [61, 62].

4.2. Effect of deposition potential

In an electrolyte of $Mn(CH_3COO)_2$, 0.5 V (*vs.* SCE) of anodic potential forms a manganese oxide consists of two oxidation states: trivalent (Mn^{3+}) and tetravalent states (Mn^{4+}), while divalent ions Mn^{2+} and Mn^{3+} are observed for manganese oxide formed at anodic potential lower than 0.5 V [63, 64]. The manganese oxide resulted from deposition potential of 0.2 V (*vs.* SCE) for 1 hour consists of γ-Mn_2O_3 and/or Mn_3O_4 while the phase transforms from tetragonal to hexagonal system when the deposition potential increased to 0.4 V and higher potentials. At anodic potential higher than 0.5 V, Mn^{4+} state becomes dominant and hydrous MnO_2 can be formed [65].

The anodic potential is found to be correlated to the adsorbed water content in the manganese oxide structure. The increase in anodic deposition potential leads to the formation of higher oxidation state of manganese ions, at the same time results in the reduction in adsorbed water content [64, 66]. As the rate of nucleus formation increases more rapidly than the rate of crystal growth with the increase of anodic potential, the morphology preferably grows horizontally, which subsequently forms a compact and layered structure. The formation of this structure is resulted from the local fluctuation of reactants. As the reactant consumption rate increases with higher deposition potential, the reactions take place at the vicinity of electrode also occur rapidly. The release of adsorbed water molecules further resulted in the formation of an uneven surface. The highest specific capacitance obtained is 240 F g^{-1} at 5 mV s^{-1}. A similar specific capacitance value is achieved when the technique applied is cathodic potentiostatic electrodeposition. The MnO_2 prepared through cathodic reduction process at a constant potential of 0.55 V (*vs.* SCE) has achieved around 233 F g^{-1} [67]. However, instead of a smooth surface which is produced at 0.5 V (*vs.* SCE) of anodic potential, a rough surface is formed for this cathodic potentiostatic electrodeposition. A further decrease in deposition potential (−1.8 V) can result in a porous structure with nanowall architecture [68].

For cathodic deposition, the increase in deposition potential leads to the uniform distribution of manganese ions onto the substrate. At relatively low cathodic deposition potential, the morphology formed is a cluster-like structure. The increase of cathodic deposition potential from −0.4 V to −0.1 V motivates the formation of flaky-like structure [62]. Further increase in cathodic deposition potential forms a more homogenous and flat structure. The formation of various structures with the cathodic deposition potential arises from the different deposition mechanisms with different potential values. The first mechanism takes place in the cathodic potential range of 0.1−0.4 V whereby the MnO_4^{2-} produced will form $H_2MnO_4^-$ that

subsequently reduce to form manganese oxide, as shown in **Reaction 7**. Another mechanism occurs at cathodic potential less than 0.2 V. It takes into account of the dissolution of manganese oxide that has formed initially. This brings about the formation of Mn^{2+} which is then reacted with MnO_4^- to produce manganese oxide, as described in **Reactions 8** and **9**.

$$3Mn^{2+} + 2MnO_4^- + 2H_2O \rightarrow 5MnO_2 + 4H^+ \quad (7)$$

$$3MnO_4^{3-} + 8H^+ \leftrightarrow MnO_4^- + 2MnO_2 + 4H_2O \quad (8)$$

$$H_2MnO_4^- + e^- \rightarrow 2MnO_2 + 4OH^- \quad (9)$$

Depending on the potential range, a potentiodynamic deposition can produce a nanorod-like structure with various diameters, given that a same scan rate is employed, as shown in **Figure 9**. Smaller potential range (0.1−0.4 V *vs.* SCE) leads to the formation of nanorods structure with higher diameter while wider potential range (0.1−0.6 V *vs.* SCE) tends to form a nanowire structure, which has relatively smaller diameter compared to nanorods [69]. Other studies that applying a small potential range (0.3−0.6 V *vs.* SCE) also led to the formation of nanorod structure with similar diameter, that is around 30 nm in average [70]. This suggests the tendency to form nanorod structured manganese oxide at 0.3 V of potential range in electrolyte consisting manganese acetate and sodium sulfate. The specific capacitances estimated from charge–discharge at 0.1 mA cm^{-2} for nanorods formed in the potential ranges of (0.1−0.4) V and (0.3−0.6) V are in the range of 200 to 250 F g^{-1}. The extension of deposition potential range from 0.3 to 0.5 V not only improves the surface area, at the same time it also enhances the specific capacitance for 44%.

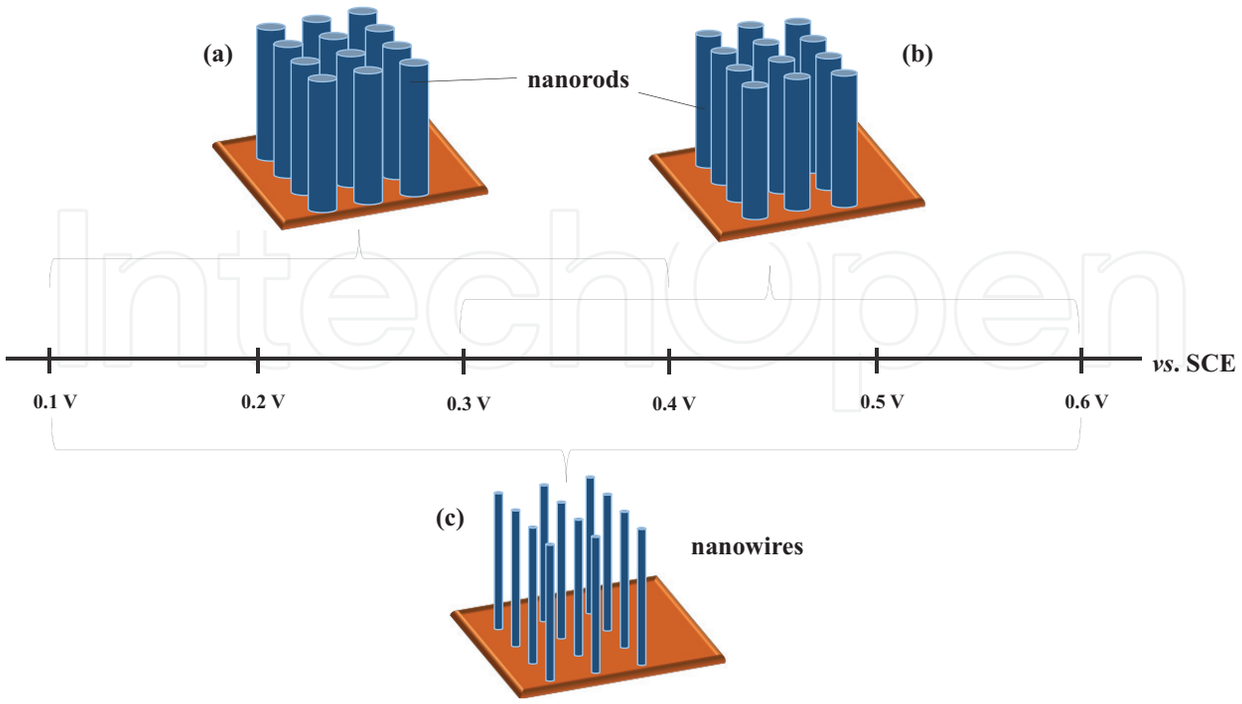

Figure 9. Morphologies formed at different potential range.

Although the integration with other materials shown enhancement in charge storage, the incorporation of carbon nanotubes (CNT) does not always work in this way. As the sp^2 carbon basal plane has low chemical and electrochemical reactivity, the nucleation sites on the surface of CNT-manganese oxide composite film are limited. In addition, the manganese oxide particles tend to grow at the CNT's junction [71]. A flower-like morphology built up by nanosheets that are originated radially from a central is thus formed. Nevertheless, this composite indeed acquires better cycle stability due to CNT acting as a conductive backbone that reduces the dissolution of particles. There is a variety of substrates can be used for deposition. Tantalum (Ta) foil has high melting point and provides good corrosion resistance, strength, and ductility. Cotton sheet supplies flexibility and textile structure that eases a uniform coating of material. Nickel (Ni) foil contributes a good electrical conductivity while the stainless steel is inert and owns a stable passivity. As a metal substrate, Ta foil and Ni foil usually offer a good cycle stability and specific capacitance of around 413 F g^{-1} in average for CNT-manganese oxide film [72, 73]. In spite of the fact that stainless steel has poorer electrical conductivity compared to other metals, the CNT-manganese oxide film composite film formed on stainless steel was found to achieve higher specific capacitance, that is 869 F g^{-1} [74]. Meanwhile, it also has good cycle stability. Given a similar morphology, which is nanowires-structured manganese oxide coated on CNT, formed on these three substrates, the distinct specific capacitance value achieved suggests the hidden advantages of stainless steel as a substrate. Direct deposition of manganese oxide on CNT paper using potentiodynamic method gives rise to around 168 F g^{-1} [70]. It is therefore important to choose an appropriate substrate for optimal electrochemical performance. Without the CNT, the manganese oxide tends to appear in nanorod-like structure and sphere-like structure at oxidation condition and reduction condition, respectively [75]. For the manganese oxide deposited within the same potential range (0.1−0.4 V), a desired structure can be determined by applying different annealing temperatures. For example, 300°C leads to the formation of nanotubes structure while 100°C forms nanorods structure [76]. The manganese oxide-based films prepared at different scan rates during potentiodynamic deposition possess distinct morphologies. At scan rate lower than 100 mV s^{-1}, the morphology forms are irregular and dense. It starts to evolve and becomes more porous when the scan rate of deposition is increased. A nanoflake structure can be formed at scan rate of 200 mV s^{-1} [77]. This structure is beneficial for charge storage purpose at which it has offered specific capacitance of 410 F g^{-1}. The compact and non-porous structure produced at relatively scan rate achieved around 150 F g^{-1}.

4.3. Effect of deposition current density

Potentiostatic deposition tends to form a more compact structure compared to the galvanostatic deposition. This is due to the consistent deposition rate during potentiostatic deposition. As the potential is maintained throughout the deposition process, the deposition rate is sustained. In contrast, the potential varies during galvanostatic deposition in order to sustain the current supply. The structure formed is thus less compact and higher in surface area [78]. The difference in compactness contributes to 50% increment in specific capacitance value and 15% higher capacitance retention upon 5000 cycles for galvanostatic deposited manganese oxide film. During the galvanostatic deposition, the structure changes from irregular to regular

and uniform structure with the increased in current density [79, 80]. When the current density exceeds the optimal value to deposit Mn^{4+}, a clustered structure which consists of soluble Mn^{6+} and/or Mn^{7+} may forms. Other than oxidation states, the morphology also changes with current density. The evolution of morphology is easily observed using field emission scanning electron microscopy (FESEM). As the nucleation rate is directly related to the current density, a lower current density produces lower nucleation rate. As a result, there is not many nuclei formed on the substrate surface and a continuous deposit layer is hard to be constructed [81]. In addition, the deposit usually possesses rough surface. Higher current density can lead to higher nucleation and growth rate. The deposit accumulates on the structure formed ahead and filling up the space or crack, which leads to the formation of a uniform coating, **Figure 10**.

At optimal current density, various structures such as nanowires, nanoflakes, nanosheets, and nanorods can be formed [57, 82, 83]. For example, manganese oxide formed from $MnSO_4$ precursor at 4 mA cm^{-2} presents as agglomerated clusters. A small decreased in current density, 3.7 mA cm^{-2}, brings about a grain-like structure constructed by nanowires [84]. 2 mA cm^{-2} of galvanostatic deposition in $Mn(NO_3)_2$ produces a flower-like structure made up of nanowires [83]. This manganese oxide film is capable to maintain 84% of specific capacitance after 1000 cycles.

4.4. Electrophoretic deposition

As one kind of the electrodeposition techniques, the oxidation and dissolution of the metal substrate during the anodic electrophoretic deposition is a concern. Thus, cathodic electrophoretic deposition is more favorable compared to its counterpart. Different from the electrodeposition techniques mentioned above, the electrophoretic deposition does not form the oxide during or after the process. Instead, the oxide is fabricated beforehand. The desired nanostructure can be manipulated using various preparation methods such as hydrothermal, chemical reduction, chemical precipitation, spray pyrolysis, and wet-chemical processes. The nanostructured oxide powder formed is then suspended in a dispersant electrolyte for further action, which is the electrophoretic deposition in this case. The structure of manganese oxide particles will be retained even after deposition, as depicted in **Figure 11**.

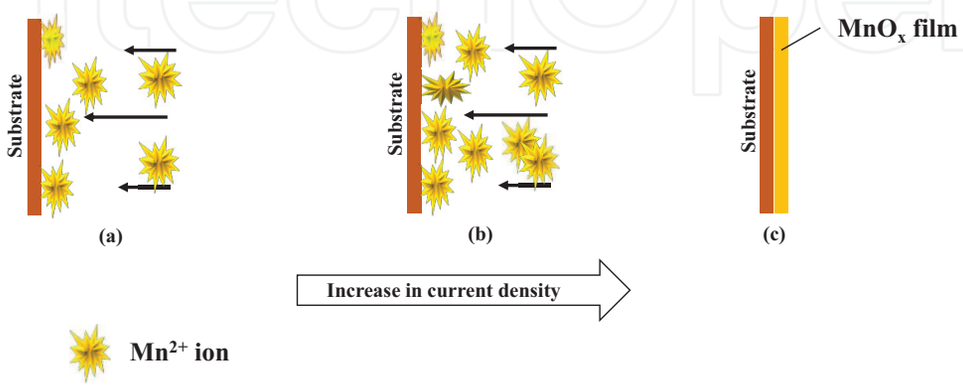

Figure 10. Morphological evolution with the increase in current density.

http://dx.doi.org/10.5772/intechopen.71957

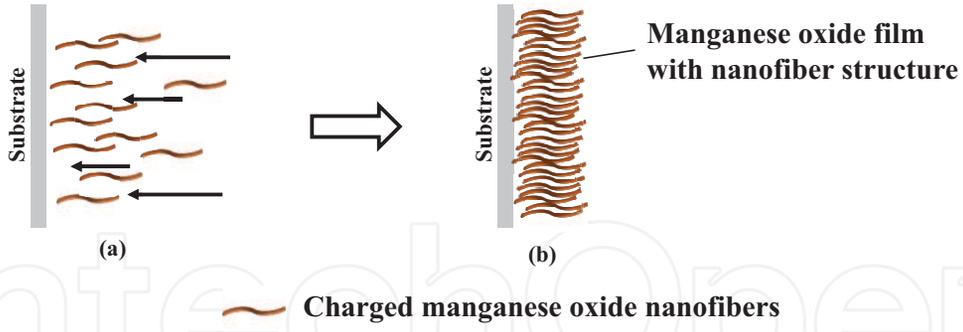

Figure 11. Schematic diagram of electrophoretic deposited manganese oxide film.

It can be seen that the stability of manganese oxide suspension is important to ensure the success of electrophoretic deposition. The ethanol can be used as the liquid medium for suspension. However, the deposit resulted from the manganese oxide suspension in ethanol is shown to be irregular and tends to form agglomerates. The addition of phosphate ester has been shown to enhance the stability of the manganese oxide suspension and increase the mass load [85]. This improves the electrochemical performance of the manganese oxide film. Without the phosphate ester, the manganese oxide film only exhibits 236 F g^{-1} of specific capacitance and drops 15% of the initial specific capacitance after 25 cycles [86]. Meanwhile, the phosphate ester has offered around 60% of increment in specific capacitance [85]. Sodium alginate is a good dispersant as well. It has been proposed that the sodium alginate provides the electrostatic and steric stabilization for the manganese oxide suspension. Additionally, it supplies electric charge for the suspension particles which is beneficial for the deposition process [87]. The manganese oxide film deposited from the dispersant electrolyte of sodium alginate has obtained specific capacitance (412 F g^{-1}) a little higher than the one prepared from the ethanol with phosphate ester dispersant electrolyte (377 F g^{-1}). The integration of carbon nanotubes or reduced graphene oxide with the manganese oxide does not alter the nanostructure of the oxide itself [88]. The nanostructured manganese oxide particles attach on the carbon nanotube surface and deposit together onto the substrate [89].

We have discussed about the impact of few deposition parameters on the deposited manganese oxide-based film. The as-deposited manganese oxide-based film is dominantly amorphous with inherent cation deficiency [90]. The defect is most likely to form at relatively low deposition temperatures (80−200°C). Except the one prepared using electrophoretic deposition, at which the manganese oxide particles are firstly fabricated before deposition, the as-deposited manganese oxide-based film requires certain post-treatments to improve the crystalline structure. Annealing is one of the common post-treatment. When the manganese oxide-based film undergoes post-heating process, different crystalline structure forms based on the annealing temperature. Most of the water content at the surface layer of structure desorbs gradually at 120−350°C [91]. The manganese oxide presents as γ-manganese oxide at annealing temperature lower than 350°C. The transformation of crystalline structure is initiated at around 300°C, which allows the γ-phase changes to β-phase of MnO_2. When the manganese oxide undergoes further heating, α-Mn_2O_3 phase starts to form [92]. Any desired crystalline structure is thus can be prepared. Other than crystalline structure, the morphology

Figure 12. Morphologies of manganese oxide film formed at annealing temperature of (a) 100 – 200°C, (b) 300°C, (c) 500°C, and (d) 600°C.

of the manganese oxide-based film can also be modified by varying the annealing temperatures. At annealing temperatures lower than 200°C, a fibrous and granular structure is formed. The entanglement of fibers causes the morphology to evolve to a cluster-like structure when the temperature reaches 300°C. Further increasing in temperature can lead to the formation of flaky-like (500°C) and rod-like structures (600°C) [93], **Figure 12**.

There are still many studies carried out to investigate other possible factors affecting the deposited manganese oxide-based film. For example, by studying the porosity of the manganese oxide-based film, one can also inspect more details about the structure and charge transport properties [94]. More and more deposition techniques have been developed and studied to prepare the manganese oxide-based film. For instance, a redox deposition that is took place when a substrate is immersed substrate into the Mn ions precursors [95, 96]. From chemical bath deposition, chemical vapor deposition to spray pyrolysis deposition, all deposition techniques are intended to grow the deposit with a good quality along with good physical and chemical properties in a large scale.

5. Summary

Manganese oxide-based film is shown to be prepared in various electrodeposition conditions by varying electrodeposition potentials, current densities, additives, and electrolytes. The potential application of manganese oxide-based film as the electrode material for electrochemical capacitor is thus discussed. As deposited manganese oxide film is amorphous in nature [97], the amorphousness can be transformed to crystalline phase by employing appropriate annealing temperature. The crystallinity start to arise when the annealing temperature increases to 300°C. MnO_2 is the first crystal structure detected at 300°C, further increasing the temperature leads to the formation of Mn_3O_4 and Mn_2O_3 [98]. Since proton participates in the charge storage mechanism of manganese oxide, it is believed that this oxide will perform better in hydrous form. Previous study about the RuO_2 has shown the significant improvement on the electrochemical performance with the presence of hydrous phase [99]. Not long after that, the crystalline manganese oxide has exhibited its potential application as electrode material as well [12]. To date, the charge storage mechanism is found to be dependent on the crystalline structure, water content, and surface area. It turns out that, the electrochemical performance of manganese oxide-based film is not totally relied on any of these factors. In contrast, it is resulted from the combination of all the factors that have been found and studied. For this reason, the researchers are still making effort to understand this complication.

The addition of secondary or ternary materials can enhance the electrochemical performance of manganese oxide film. However, these are not shown in this chapter. The core idea is to gather the advantages of various materials then compensate shortcomings of each other. The common materials combination involves the carbon material, transition metal oxide, and conducting polymer. The carbon material offers conductivity while transition metal oxide and conducting polymer provides more electroactive sites for charge storage purpose. Electrodeposition is a widely used technique to protect and strengthen the function of parts used in various industries. The wide application of electrodeposition technology can be attributed to its simplicity, manufacturability, and scalability. The electrodeposition method also requires a relatively low fabrication cost for energy storage device compared to other methods. This technique allows a direct formation of film on the substrate desired and the film properties are governable by varying the deposition parameters. The traditional method of electrode fabrication for electrochemical capacitor involves the pressing of electrode material onto the substrate. This process can increase the contact resistance and reduce the porous surface area which brings about damage to the electrode materials formed. In overall, manganese oxide-based film prepared using electrodeposition is prospective and practical. There are numerous related studies carrying out every year, although the reported specific capacitance of manganese oxide-based film are yet far from the expected performances (**Table 1**), we are convinced that there is still a big room for improvement.

Electrode materials	Deposition mode		Deposition electrolyte	Specific capacitance, F g^{-1}	Reference
MnO_x	Potentiostatic	0.2 V *vs*. SCE	0.001 M $KMnO_4$ + 1 M Na_2SO_4	368.00	[62]
MnO_x	Potentiostatic	0.50 V *vs*. SCE	0.25 M $Mn(CH_3COO)_2$	240.00	[63]
MnO_2	Potentiostatic	0.55 V *vs*. SCE	$KMnO_4$	232.94	[67]
a-$MnO_2{\cdot}nH_2O$	Potentiostatic	0.75 V *vs*. SCE	0.25 M $MnSO_4{\cdot}5H_2O$	285.00	[65]
MnO_x	Potentiostatic	1.0 V *vs*. Ag/AgCl	2 mM $MnSO_4$ + 50 mM KCl	163.40	[44]
MnO_x	Potentiostatic	1.1 V *vs*. Ag/AgCl	0.1 M $MnSO_4$ + 0.01 M TTAB	343.00	[100]
MnO_x			0.1 M $MnSO_4$	294.00	
MnO_2	Potentiostatic	10 V *vs*. Ag/AgCl	0.5 M $KMnO_4$	128.00	[78]
Mn_3O_4	Potentiostatic	−1.3 V *vs*. SCE	0.25 M $MnNO_3$	416.00	[101]
MnO_2	Potentiostatic	0.60 *vs*. SCE	0.1 M $Mn(CH_3COO)_2$ + 0.1 M Na_2SO_4	240.00	[102]
MnO_2-CNT	Cyclic voltammetry	0.30–0.60 V *vs*. SCE		167.50	[70]
Mn-Ni mixed oxide	Cyclic voltammetry	0.4 − 1.2 V *vs*. Ag/AgCl	0.05 M $Mn(CH_3COO)_2$ + 0.1 M $Ni(CH_3COO)_2$ + 0.2 M CH_3COONa	169.00	[103]
Mn-Mo mixed oxide	Cyclic voltammetry	0.00 − 1.00 V *vs*. Ag/AgCl	2 mM $MnSO_4$ + 20 mM Na_2MoO_4	190.90	[104]
MnO_x	Cyclic voltammetry	1.10 − 1.50 V *vs*. SCE	0.5 M $MnSO_4$ + 0.5 M Na_2SO_4 + 100 mM SLS	310.00	[105]

Electrode Materials	Deposition mode		Electrolyte composition	Specific capacitance, F g^{-1}	Reference
MnO_2	Galvanostatic	2 mA cm^{-2}	5 mM $Mn(NO_3)_2$	246.00	[83]
MnO_2	Galvanostatic	3 mA cm^{-2}	0.02 M $KMnO_4$	188.00	[106]
MnO_2-PPy	Galvanostatic	4 mA cm^{-2}	0.2 M $MnSO_4$ + PPy	620.00	[84]
Fe-doped MnO_x	Galvanostatic	5 mA cm^{-2}	0.1 M $MnSO_4$ + 0.1 M citric acid	218.00	[107]
MnO_x	Galvanostatic	5 mA cm^{-2}	0.01 M $Mn(CH_3COO)_2$	185.00	[57]
MnO_2	Galvanostatic	10.5 mA cm^{-2}	0.02 M $Mn(CH_3COO)_2$	201.00	[108]
Co-doped MnO_x	Galvanostatic	50 mA cm^{-2}	MnSO4, cobalt sulfate, EDTA	186.20	[109]
Fe-doped MnO_x	Galvanostatic		MnSO4, iron sulfate, EDTA	298.40	
MnO_2	Galvanostatic	165 mA cm^{-2}	0.5 M $KMnO_4$	196.00	[78]
MnO_2-RGO	Electrophoretic deposition	0.3 V *vs.* SCE	MnO_2 + RGO	392.00	[88]
MnO_X	Electrophoretic deposition	5 − 10 V *vs.* SCE	Manganese oxide + sodium alginate	412.00	[87]
MnO_x	Electrophoretic deposition	10 − 100 V *vs.* SCE	Manganese oxide + ethanol + phosphate ester	377.00	[85]
MnO_x-CNT	Electrophoretic deposition	15 V *vs.* SCE	Manganese oxide + sodium alginate + carbon nanotubes	Around 210.00	[89]
MnO_x	Electrophoretic deposition	100 V *vs.* Ag/AgCl	Manganese oxide + ethanol	236.00	[86]
MnO_x	Electrophoretic deposition	100 V *vs.* Ag/AgCl	Manganese oxide + ethylene alcohol + H_2SO_4	275.00	[110]

Table 1. The electrochemical performance of deposited manganese oxide-based film.

Acknowledgements

The authors acknowledge the University of Malaya for providing financial support through the projects BKS030-2017 and FG034-17AFR.

Author details

Chan Pei Yi and Siti Rohana Majid*

*Address all correspondence to: shana@um.edu.my

Centre for Ionics University of Malaya, Department of Physics, Faculty of Science, University of Malaya, Kuala Lumpur, Malaysia

References

[1] Ogden JM, Steinbugler MM, Kreutz TG. A comparison of hydrogen, methanol and gasoline as fuels for fuel cell vehicles: Implications for vehicle design and infrastructure development. Journal of Power Sources. 1999;**79**(2):143-168

[2] Lai JS, Nelson DJ. Energy management power converters in hybrid electric and fuel cell vehicles. Proceedings of the IEEE. 2007;**95**(4):766-777

[3] Garcia P, Fernandez LM, Garcia CA, Jurado F. Energy management system of fuel-cell-battery hybrid tramway. IEEE Transactions on Industrial Electronics. 2010;**57**(12):4013-4023

[4] Tsukahara K, Kondo K. A Study on Methods to Design and Select Energy Storage Devices for Fuel Cell Hybrid Powered Railway Vehicles. Paper presented at the IECON 2013-39th Annual Conference of the IEEE Industrial Electronics Society; 2013, 10-13 Nov. 2013

[5] Abraham KM. Prospects and limits of energy storage in batteries. Journal of Physical Chemistry Letters. 2015;**6**(5):830-844

[6] Braga MH, Grundish NS, Murchison AJ, Goodenough JB. Alternative strategy for a safe rechargeable battery. Energy & Environmental Science. 2017;**10**(1):331-336

[7] Ragone DV. Review of Battery Systems for Electrically Powered Vehicles; 1968

[8] McCloskey BD. Expanding the Ragone plot: Pushing the limits of energy storage. Journal of Physical Chemistry Letters. 2015;**6**(18):3592-3593

[9] Conway BE. Electrochemical Supercapacitors: Scientific Fundamentals and Technological Applications. US: Springer; 1999

[10] Zheng JP, Cygan PJ, Jow TR. Hydrous ruthenium oxide as an electrode material for electrochemical capacitors. Journal of the Electrochemical Society. 1995;**142**(8):2699-2703

[11] Brezesinski T, Wang J, Polleux J, Dunn B, Tolbert SH. Templated Nanocrystal-based porous TiO_2 films for next-generation electrochemical capacitors. Journal of the American Chemical Society. 2009;**131**(5):1802-1809

[12] Brousse T, Toupin M, Dugas R, Athouël L, Crosnier O, Bélanger D. Crystalline MnO_2 as possible alternatives to amorphous compounds in electrochemical supercapacitors. Journal of the Electrochemical Society. 2006;**153**(12):A2171-A2180

[13] Deng L, Zhang G, Kang L, Lei Z, Liu C, Liu Z-H. Graphene/VO_2 hybrid material for high performance electrochemical capacitor. Electrochimica Acta. 2013;**112**:448-457

[14] Li F, Song J, Yang H, Gan S, Zhang Q, Han D, et al. One-step synthesis of graphene/SnO_2 nanocomposites and its application in electrochemical supercapacitors. Nanotechnology. 2009;**20**(45):455602

[15] Xiao X, Ding T, Yuan L, Shen Y, Zhong Q, Zhang X, et al. WO3−x/MoO3−x Core/Shell nanowires on carbon fabric as an anode for all-solid-state asymmetric supercapacitors. Advanced Energy Materials. 2012;**2**(11):1328-1332

[16] Sin D-Y, Koo B-R, Ahn H-J. Hollow lithium manganese oxide nanotubes using MnO_2-carbon nanofiber composites as cathode materials for hybrid capacitors. Journal of Alloys and Compounds. 2017;**696**:290-294

[17] Unnikrishnan B, Wu C-W, Chen IWP, Chang H-T, Lin C-H, Huang C-C. Carbon dot-mediated synthesis of manganese oxide decorated graphene nanosheets for supercapacitor application. ACS Sustainable Chemistry & Engineering. 2016;**4**(6): 3008-3016

[18] Wang Y, Zhitomirsky I. Cathodic electrodeposition of Ag-doped manganese dioxide films for electrodes of electrochemical supercapacitors. Materials Letters. 2011;**65** (12):1759-1761

[19] Maynard JB. The chemistry of manganese ores through time: A signal of increasing diversity of earth-surface environments. Economic Geography. 2010;**105**(3):535-552

[20] Augustin M, Fenske D, Bardenhagen I, Westphal A, Knipper M, Plaggenborg T, et al. Manganese oxide phases and morphologies: A study on calcination temperature and atmospheric dependence. Beilstein Journal of Nanotechnology. 2015;**6**:47-59

[21] Feng Q, Kanoh H, Ooi K. Manganese oxide porous crystals. Journal of Materials Chemistry. 1999;**9**(2):319-333

[22] Jia M-Y, Xu B, Ding X-L, He S-G, Ge M-F. Experimental and theoretical study of the reactions between manganese oxide cluster anions and hydrogen sulfide. Journal of Physical Chemistry C. 2012;**116**(45):24184-24192

[23] Kulp JL, Perfetti JN. Thermal study of some manganese oxide minerals. Mineralogical Magazine. 1950;**29**(210):239-252

[24] Mande C, Deshpande AP. A study of manganese oxides by EXAFS spectroscopy. Physica Status Solidi (b). 1990;**158**(2):737-742

[25] Post JE. Manganese oxide minerals: Crystal structures and economic and environmental significance. Proceedings of the National Academy of Sciences of the United States of America. 1999;**96**(7):3447-345 4

[26] Tian Z-R, Tong W, Wang J-Y, Duan N-G, Krishnan VV, Suib SL. Manganese oxide mesoporous structures: Mixed-valent semiconducting catalysts. Sci. 1997;**276**(5314):926-930

[27] Devaraj S, Munichandraiah N. Effect of crystallographic structure of MnO_2 on its electrochemical capacitance properties. Journal of Physical Chemistry C. 2008;**112**(11):4406-4417

[28] Bigliocca C, Girardi F, Pauly J, Sabbioni E, Meloni S, Provasoli A. Radiochemical separations by adsorption on manganese dioxide. Analytical Chemistry. 1967;**39**(13):1634-1639

[29] Li L, Xu J, Zheng X, Ma C, Song X, Ge S, et al. Growth of gold-manganese oxide nanostructures on a 3D origami device for glucose-oxidase label based electrochemical immunosensor. Biosensors & Bioelectronics. 2014;**61**:76-82

[30] Li X, Hu B, Suib S, Lei Y, Li B. Manganese dioxide as a new cathode catalyst in microbial fuel cells. Journal of Power Sources. 2010;**195**(9):2586-2591

[31] Loganathan P, Burau RG. Sorption of heavy metal ions by a hydrous manganese oxide. Geochimica et Cosmochimica Acta. 1973;**37**(5):1277-1293

[32] Piispanen JK, Sallanko JT. Mn(II) removal from groundwater with manganese oxide-coated filter media. Journal of Environmental Science and Health, Part A. 2010;**45**(13): 1732-1740

[33] Smith PF, Deibert BJ, Kaushik S, Gardner G, Hwang S, Wang H, et al. Coordination geometry and oxidation state requirements of corner-sharing MnO_6 octahedra for water oxidation catalysis: An investigation of manganite (γ-MnOOH). ACS Catalysis. 2016;**6**(3): 2089-2099

[34] Thackeray MM. Manganese oxides for lithium batteries. Progress in Solid State Chemistry. 1997;**25**(1):1-71

[35] Pourbaix M. Atlas of Electrochemical Equilibria in Aqueous Solutions Retrieved from ElectronicBooks database; 1974

[36] Pang SC, Anderson MA, Chapman TW. Novel electrode materials for thin film ultracapacitors: Comparison of electrochemical properties of sol gel derived and electrodeposited manganese dioxide. Journal of the Electrochemical Society. 2000;**147**(2):444-450

[37] Dupont M, Hollenkamp AF, Donne SW. Electrochemically active surface area effects on the performance of manganese dioxide for electrochemical capacitor applications. Electrochimica Acta. 2013;**104**:140-147

[38] Ghaemi M, Ataherian F, Zolfaghari A, Jafari SM. Charge storage mechanism of sonochemically prepared MnO_2 as supercapacitor electrode: Effects of physisorbed water and proton conduction. Electrochimica Acta. 2008;**53**(14):4607-4614

[39] Toupin M, Brousse T, Bélanger D. Influence of microstucture on the charge storage properties of chemically synthesized manganese dioxide. Chemistry of Materials. 2002;**14**(9): 3946-3952

[40] Wu T-H, Hesp D, Dhanak V, Collins C, Braga F, Hardwick LJ, Hu C-C. Charge storage mechanism of activated manganese oxide composites for pseudocapacitors. Journal of Materials Chemistry A. 2015;**3**(24):12786-12795

[41] Ahmed KAM, Peng H, Wu K, Huang K. Hydrothermal preparation of nanostructured manganese oxides (MnOx) and their electrochemical and photocatalytic properties. Chemical Engineering Journal. 2011;**172**(1):531-539

[42] Aref AA, Tang YW. Chemical bath deposition synthesis and electrochemical properties of MnO_2 thin film: Effect of deposition time and bath temperature. Materials Science-Poland. 2014;**32**(4):555-564

[43] Lee SW, Kim J, Chen S, Hammond PT, Shao-Horn Y. Carbon nanotube/manganese oxide ultrathin film electrodes for electrochemical capacitors. ACS Nano. 2010;**4**(7):3889-3896

[44] Nakayama M, Kanaya T, Inoue R. Anodic deposition of layered manganese oxide into a colloidal crystal template for electrochemical supercapacitor. Electrochemistry Communications. 2007;**9**(5):1154-1158

[45] Ni J, Lu W, Zhang L, Yue B, Shang X, Lv Y. Low-temperature synthesis of monodisperse 3D manganese oxide nanoflowers and their pseudocapacitance properties. Journal of Physical Chemistry C. 2009;**113**(1):54-60

[46] Stumm W, Morgan JJ. Aquatic chemistry: an introduction emphasizing chemical equilibria in natural waters (pp. 795-795); 1981

[47] Wang Y, Zhitomirsky I. Electrophoretic deposition of manganese dioxide−multiwalled carbon nanotube composites for electrochemical supercapacitors. Langmuir. 2009;**25**(17):9684-9689

[48] Xiao XF, Liu RF. Effect of suspension stability on electrophoretic deposition of hydroxyapatite coatings. Materials Letters. 2006;**60**(21–22):2627-2632

[49] Besra L, Liu M. A review on fundamentals and applications of electrophoretic deposition (EPD). Progress in Materials Science. 2007;**52**(1):1-61

[50] Zhitomirsky I. Cathodic electrodeposition of ceramic and organoceramic materials. Fundamental aspects. Advances in Colloid and Interface Science. 2002;**97**(1–3):279-317

[51] Zhitomirsky I, Cheong M, Wei J. The cathodic electrodeposition of manganese oxide films for electrochemical supercapacitors. JOM. 2007;**59**(7):66-69

[52] Chen Y-S, Hu C-C, Wu Y-T. Capacitive and textural characteristics of manganese oxide prepared by anodic deposition: Effects of manganese precursors and oxide thickness. Journal of Solid State Electrochemistry. 2004;**8**(7):467-473

[53] Rangappa KS, Chandraju D, Made Gowda NM. Oxidation of L-glutamine by manganese (III) in aqueous sulfuric acid, acetic acid, and pyrophosphate media: A kinetic and mechanistic study. International Journal of Chemical Kinetics. 1998;**30**:7-19

[54] Guidelli R, Piccardi G. The voltammetric behaviour of the Mn2+, Mn3+, Mn4+ system in 15 N H2SO4 on a smooth platinum microelectrode. Electrochimica Acta. 1968;**13**(1):99-107

[55] Kao W-H, Weibel VJ. Electrochemical oxidation of manganese(II) at a platinum electrode. Journal of Applied Electrochemistry. 1992;**22**(1):21-27

[56] Fleischmann M, Thirsk HR, Tordesillas IM. Kinetics of electrodeposition of γ-manganese dioxide. Transactions of the Faraday Society. 1962;**58**(0):1865-1877

[57] Babakhani B, Ivey DG. Anodic deposition of manganese oxide electrodes with rod-like structures for application as electrochemical capacitors. Journal of Power Sources. 2010;**195**(7):2110-2117

[58] Dupont MF, Donne SW. Nucleation and growth of electrodeposited manganese dioxide for electrochemical capacitors. Electrochimica Acta. 2014;**120**:219-225

[59] Cross A, Morel A, Cormie A, Hollenkamp T, Donne S. Enhanced manganese dioxide supercapacitor electrodes produced by electrodeposition. Journal of Power Sources. 2011;**196**(18):7847-7853

[60] Clarke CJ, Browning GJ, Donne SW. An RDE and RRDE study into the electrodeposition of manganese dioxide. Electrochimica Acta. 2006;**51**(26):5773-5784

[61] Broughton JN, Brett MJ. Variations in MnO_2 electrodeposition for electrochemical capacitors. Electrochimica Acta. 2005;**50**(24):4814-4819

[62] Gibson AJ, Latham KG, Burns RC, Donne SW. Electrodeposition mechanism of cathodically-prepared manganese dioxide thin films from permanganate for use in electrochemical capacitors. Electrochimica Acta. 2017;**236**:198-211

[63] Chang J-K, Tsai W-T. Material characterization and electrochemical performance of hydrous manganese oxide electrodes for use in electrochemical pseudocapacitors. Journal of the Electrochemical Society. 2003;**150**(10):A1333-A1338

[64] Chigane M, Ishikawa M. Manganese oxide thin film preparation by potentiostatic electrolyses and electrochromism. Journal of the Electrochemical Society. 2000;**147**(6): 2246-2251

[65] Hu C-C, Tsou T-W. Ideal capacitive behavior of hydrous manganese oxide prepared by anodic deposition. Electrochemistry Communications. 2002;**4**(2):105-109

[66] Rodrigues S, Shukla AK, Munichandraiah N. A cyclic voltammetric study of the kinetics and mechanism of electrodeposition of manganese dioxide. Journal of Applied Electrochemistry. 1998;**28**(11):1235-1241

[67] Yuqiu H, Hongcheng Z. Cathodic potentiostatic electrodeposition and capacitance characterization of manganese dioxide film. Energy Procedia. 2011;**11**:2769-2774

[68] Liu D, Garcia BB, Zhang Q, Guo Q, Zhang Y, Sepehri S, Cao G. Mesoporous hydrous manganese dioxide nanowall arrays with large lithium ion energy storage capacities. Advanced Functional Materials. 2009;**19**(7):1015-1023

[69] Wu M-S. Electrochemical capacitance from manganese oxide nanowire structure synthesized by cyclic voltammetric electrodeposition. Applied Physics Letters. 2005;**87**(15): 153102

[70] Chou S-L, Wang J-Z, Chew S-Y, Liu H-K, Dou S-X. Electrodeposition of MnO_2 nanowires on carbon nanotube paper as free-standing, flexible electrode for supercapacitors. Electrochemistry Communications. 2008;**10**(11):1724-1727

[71] Zhang H, Cao G, Wang Z, Yang Y, Shi Z, Gu Z. Growth of manganese oxide nanoflowers on vertically-aligned carbon nanotube arrays for high-rate electrochemical capacitive energy storage. Nano Letters. 2008;**8**(9):2664-2668

[72] Hu L, Chen W, Xie X, Liu N, Yang Y, Wu H, et al. Symmetrical MnO_2–carbon nanotube–textile nanostructures for wearable pseudocapacitors with high mass loading. ACS Nano. 2011;**5**(11):8904-8913

[73] Lee CY, Tsai HM, Chuang HJ, Li SY, Lin P, Tseng TY. Characteristics and electrochemical performance of Supercapacitors with manganese oxide-carbon nanotube nanocomposite electrodes. Journal of the Electrochemical Society. 2005;**152**(4):A716-A720

[74] Bordjiba T, Bélanger D. Development of new nanocomposite based on nanosized-manganese oxide and carbon nanotubes for high performance electrochemical capacitors. Electrochimica Acta. 2010;**55**(9):3428-3433

[75] Ashassi-Sorkhabi H, Asghari E, La'le Badakhshan P. Potentiostatic and cyclic voltammetric deposition of nanostructured manganese oxide for supercapacitor applications. Current Applied Physics. 2014;**14**(2):187-191

[76] Wu M-S, Lee J-T, Wang Y-Y, Wan C-C. Field emission from manganese oxide nanotubes synthesized by cyclic voltammetric electrodeposition. The Journal of Physical Chemistry. B. 2004a;**108**(42):16331-16333

[77] Prasad KR, Miura N. Potentiodynamically deposited nanostructured manganese dioxide as electrode material for electrochemical redox supercapacitors. Journal of Power Sources. 2004;**135**(1–2):354-360

[78] Ali GAM, Yusoff MM, Ng YH, Lim HN, Chong KF. Potentiostatic and galvanostatic electrodeposition of manganese oxide for supercapacitor application: A comparison study. Current Applied Physics. 2015;**15**(10):1143-1147

[79] Drosos H, Sapountzis A, Koudoumas E, Katsarakis N, Vernardou D. Effect of deposition current density on electrodeposited vanadium oxide coatings. Journal of the Electrochemical Society. 2012;**159**(8):E145-E147

[80] Guo HJ, Zhu BQ, Li XH, Zhang XM, Wang ZX, Peng WJ, Liu LP. Effects of current density on preparation of grainy electrolytic manganese dioxide. Journal of Central South University. 2005;**12**(6):667-670

[81] Babakhani B, Ivey DG. Effect of electrodeposition conditions on the electrochemical capacitive behavior of synthesized manganese oxide electrodes. Journal of Power Sources. 2011;**196**(24):10762-10774

[82] Wei W, Cui X, Mao X, Chen W, Ivey DG. Morphology evolution in anodically electrodeposited manganese oxide nanostructures for electrochemical supercapacitor applications—Effect of supersaturation ratio. Electrochimica Acta. 2011;**56**(3):1619-1628

[83] Yousefi T, Golikand AN, Mashhadizadeh MH, Aghazadeh M. Template-free synthesis of MnO_2 nanowires with secondary flower like structure: Characterization and supercapacitor behavior studies. Current Applied Physics. 2012;**12**(1):193-198

[84] Sharma RK, Rastogi AC, Desu SB. Manganese oxide embedded polypyrrole nanocomposites for electrochemical supercapacitor. Electrochimica Acta. 2008;**53**(26):7690-7695

[85] Li J, Zhitomirsky I. Cathodic electrophoretic deposition of manganese dioxide films. Colloids and Surfaces A: Physicochemical and Engineering. 2009a;**348**(1):248-253

[86] Chen C-Y, Wang S-C, Lin C-Y, Chen F-S, Lin C-K. Electrophoretically deposited manganese oxide coatings for supercapacitor application. Ceramics International. 2009;**35**(8): 3469-3474

[87] Li J, Zhitomirsky I. Electrophoretic deposition of manganese oxide nanofibers. Materials Chemistry and Physics. 2008;**112**(2):525-530

[88] Ghasemi S, Hosseinzadeh R, Jafari M. MnO_2 nanoparticles decorated on electrophoretically deposited graphene nanosheets for high performance supercapacitor. International Journal of Hydrogen Energy. 2015;**40**(2):1037-1046

[89] Li J, Zhitomirsky I. Electrophoretic deposition of manganese dioxide–carbon nanotube composites. The Journal of Materials Processing Technology. 2009b;**209**(7):3452-3459

[90] Wei W, Chen W, Ivey DG. Defective rock-salt structure in anodically electrodeposited Mn−co−O nanocrystals. Journal of Physical Chemistry C. 2007;**111**(28):10398-10403

[91] Preisler E. Semiconductor properties of manganese dioxide. Journal of Applied Electrochemistry. 1976;**6**(4):311-320

[92] Giovanoli R, Stähli E, Feitknecht W. Über oxidhydroxide des vierwertigen Mangans mit Schichtengitter 2. Mitteilung: Mangan (III)-manganat (IV). Helvetica Chimica Acta. 1970;**53**(3):453-464

[93] Chang J-K, Chen Y-L, Tsai W-T. Effect of heat treatment on material characteristics and pseudo-capacitive properties of manganese oxide prepared by anodic deposition. Journal of Power Sources. 2004;**135**(1–2):344-353

[94] Gamble T, Gillette E, Lee SB, Siwy ZS. Probing porous structure of single manganese oxide mesorods with ionic current. Journal of Physical Chemistry C. 2013;**117**(47):24836-24842

[95] George AT, Ganesan R, Thangeeswari T. Redox Deposition of Manganese Oxide Nanoparticles on Graphite Electrode by Immersion Technique for Electrochemical Super Capacitors; 2016

[96] Wu M, Snook GA, Chen GZ, Fray DJ. Redox deposition of manganese oxide on graphite for supercapacitors. Electrochemistry Communications. 2004b;**6**(5):499-504

[97] Shinomiya T, Gupta V, Miura N. Effects of electrochemical-deposition method and microstructure on the capacitive characteristics of nano-sized manganese oxide. Electrochimica Acta. 2006;**51**(21):4412-4419

[98] Nagarajan N, Humadi H, Zhitomirsky I. Cathodic electrodeposition of MnOx films for electrochemical supercapacitors. Electrochimica Acta. 2006;**51**(15):3039-3045

[99] Zheng J, Huang C. Electrochemical behavior of amorphous and crystalline ruthenium oxide electrodes. Journal of New Materials for Electrochemical Systems. 2002;**5**:41

[100] Lee H-M, Cho S-W, Song C-J, Kang HJ, Kwon BJ, Kim C-K. Abrupt change with surfactant concentration in the surface morphology of the electrodeposited manganese oxide films for electrochemical capacitors. Electrochimica Acta. 2015;**160**:50-56

[101] Nguyen T, João Carmezim M, Boudard M, Fátima Montemor M. Cathodic electrodeposition and electrochemical response of manganese oxide pseudocapacitor electrodes. International Journal of Hydrogen Energy. 2015;**40**(46):16355-16364

[102] Chou S, Cheng F, Chen J. Electrodeposition synthesis and electrochemical properties of nanostructured γ-MnO_2 films. Journal of Power Sources. 2006;**162**(1):727-734

[103] Tahmasebi MH, Raeissi K, Golozar MA, Vicenzo A, Hashempour M, Bestetti M. Tailoring the pseudocapacitive behavior of electrochemically deposited manganese-nickel oxide films. Electrochimica Acta. 2016;**190**:636-647

[104] Masaharu Nakayama AT, Sato Y, Tonosaki T, Ogura K. Electrodeposition of manganese and molybdenum mixed oxide thin films and their charge storage properties. Langmuir. 2005;**21**(13):5907-5913

[105] Devaraj S, Munichandraiah N. High capacitance of electrodeposited MnO_2 by the effect of a surface-active agent. Electrochemical and Solid-State Letters. 2005;**8**(7):A373-A377

[106] Jacob GM, Zhitomirsky I. Microstructure and properties of manganese dioxide films prepared by electrodeposition. Applied Surface Science. 2008;**254**(20):6671-6676

[107] Dubal DP, Kim WB, Lokhande CD. Galvanostatically deposited Fe: MnO_2 electrodes for supercapacitor application. Journal of Physics and Chemistry of Solids. 2012;**73**(1):18-24

[108] Kundu M, Liu L. Direct growth of mesoporous MnO_2 nanosheet arrays on nickel foam current collectors for high-performance pseudocapacitors. Journal of Power Sources. 2013;**243**:676-681

[109] Trung Dung D, Thi Thu Hang L, Thi Bich Thuy H, Thanh Tung M. Synthesis of nanostructured manganese oxides based materials and application for supercapacitor. Advances in Natural Sciences: Nanoscience and Nanotechnology. 2015;**6**(2):025011

[110] Chen C-Y, Lyu Y-R, Su C-Y, Lin H-M, Lin C-K. Characterization of spray pyrolyzed manganese oxide powders deposited by electrophoretic deposition technique. Surface and Coating Technology. 2007;**202**(4):1277-1281